

Recent Advances in Arc-linear Motors for Direct-drive Applications: A Review

Zhenbao Pan, *Member, IEEE*, Jiwen Zhao, *Senior Member, IEEE*, Shuhua Fang, *Senior Member, IEEE*,
Jinhao Cai, and Qiangren Xu

Abstract—The arc-linear motor (ALM) is a new type of special motor derived from the linear motor, which has the merits of high torque, compact structure and fast dynamic response. This kind of motor does not need a complex intermediate transmission device, it is used in some direct-drive applications for continuous rotation or limited angle motion. However, there is no systematic summary and generalization of the ALMs so far. Therefore, this paper systematically overviews the recent advances in ALMs for direct-drive systems. First, the evolution process and basic structure of the ALM are introduced. And then, various ALMs are reviewed with particular reference to motor topologies, working principle, motor performance, optimization design and control techniques. To heel, a comprehensive comparison of several typical ALMs is carried out. Finally, the application areas, main challenges and development trends of the ALMs are highlighted.

Index Terms—Arc-linear motor, Linear motor, Motor topology, Permanent magnet motor.

I. INTRODUCTION

FOR the direct-drive systems such as electromagnetic launch systems, large telescopes, and so on, the traditional driving methods mainly include the worm gear transmission, gear transmission, friction transmission and coaxial installation of servo motors. However, the worm gear transmission not only has drawbacks such as reverse clearance and elastic deformation, but also have problems like long starting and braking times, which greatly reduce the tracking accuracy of the entire drive system. Although friction transmission overcomes the weaknesses of worm gear and gear transmissions, it has disadvantages such as poor

Manuscript received April 25, 2025; revised May 26, 2025; accepted June 03, 2025. Date of publication June 25, 2025; Date of current version June 10, 2025.

This work was supported in part by the National Natural Science Foundation of China under Grants 52307049 and U23A20644, in part by the Fundamental Research Funds for the Central Universities under Grant JZ2023HG7B0243, in part by the Key Laboratory of Electric Drive and Control of Anhui Province under Grant DQKJ202403, and in part by the China Postdoctoral Science Foundation under Grant 2024M751073.

Zhenbao Pan, Jiwen Zhao, and Jinhao Cai are with School of Electrical Engineering and Automation, Hefei University of Technology, Hefei 230009, China (e-mail: pzhenbao@hfut.edu.cn; ustczjw@hfut.edu.cn; 2023170470@mail.hfut.edu.cn).

Shuhua Fang, and Qiangren Xu are with School of Electrical Engineering, Southeast University, Nanjing 210096, China (e-mail: shfang@seu.edu.cn; xqr@seu.edu.cn).

(Corresponding author: Jiwen Zhao)

Digital Object Identifier 10.30941/CESTEMS.2025.00018

transmission stiffness, low-speed crawling and slippage, which directly affect the motion stability and transmission accuracy of the whole drive system [1]-[4]. Therefore, in order to improve the motion stability and transmission accuracy of the whole drive system, a transmission based on direct-drive motor is used. However, with the increase of the diameter of drive system, the loads will increase. When traditional permanent magnet (PM) motor is used as direct-drive motor, the stator/rotor is greatly increased, which make manufacturing and assembly relatively difficult. Moreover, the mechanical stiffness gets decrease [5]-[7].

In order to address the aforementioned limitations of the traditional driving methods, a new kind of direct-drive motor named “arc-linear motor (ALM)” came into being and applied into the direct-drive servo control systems [8]-[9]. According to the different application occasions of the ALM, the ALM is usually characterized by the multi-unit stator/rotor structure. Compared with the traditional whole PM motor, the ALM with multi-unit stator/rotor structure has smaller motor volume. Depending on the application scenario, the ALM can be assembled more easily and freely. Hence, the ALM is extensively recognized as a promising candidate for some direct-drive servo applications, such as large telescopes, large antennas, and so on [10]-[11].

Nowadays, many researchers at home and abroad have designed various ALMs. According to the working principle, the ALMs can be sub-categorized into two types, which are induction ALMs [12]-[22] and synchronous ALMs. Further, the synchronous ALMs can be divided into rotor-PM, stator-PM and dual-PM (DPM) types ALMs. The rotor-PM type ALMs can be classified into radial flux ALMs [23]-[30] and axial flux ALMs [31]-[34], and tubular ALMs [35]-[40] based on flux direction. The stator-PM type ALMs can be classified into three types: The first type introduces the “double salient motor [41]-[45]” to design double salient ALMs [46]-[52]. The second type adopts the “flux reversal (FR) motor [53]-[54]” to propose some FR ALMs [55]-[61]. The last type introduces the “flux switching (FS) motor [62]-[64]” to design some FS ALMs [65]-[73]. In addition, the DPM type motors [74]-[77] is used to design some DPM type ALMs [78]-[80]. The overall categorization of the existing ALMs is illustrated in Fig. 1. However, as far as we know, there is no systematic summary and generalization of ALMs so far. Hence, this paper will present a systematic review of ALMs.

The organization of this paper is as follows. In Section II,

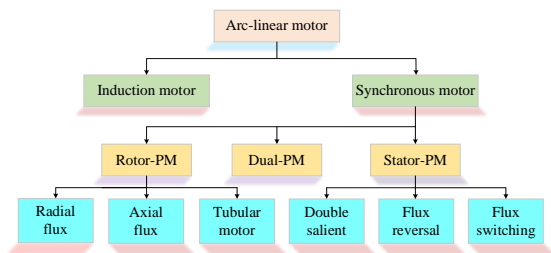


Fig. 1. Categorization of arc-linear motors.

the evolution process and basic features of ALM are described in the potential context of the direct-drive applications. Then, in Sections III-IV, various ALMs are comprehensively reviewed with particular reference to their topologies, working principles, characteristics and related advanced methods. This is followed by a comprehensive performance comparison of several typical ALMs. Subsequently, the application areas, main challenges and future trends of the ALMs are highlighted in Section V. Finally, the conclusions are drawn in Section VI.

II. EVOLUTION PROCESS AND BASIC MODELS

A. Evolution Process

This section takes a PM-ALM as an example to illustrate the evolution process of the ALM. As illustrated in Fig. 2, the PM-ALM can be evolved from the PM rotating motor. First, the PM rotating motor shown in Fig. 2(a) is cut open along the radial direction, and then the stator and rotor structures of the PM rotating motor are stretched to obtain the PM flat linear motor plotted in Fig. 2(b). At this time, the stator and rotor structures of the rotating motor become the corresponding primary and secondary structures of the flat linear motor, respectively. Then, the primary and secondary structures of the flat linear motor is bent at a certain angle, and thus the PM-ALM is finally formed, as shown in Fig. 2(c). As a special PM motor, the PM-ALM has the dual characteristics of rotating motor and linear motor.

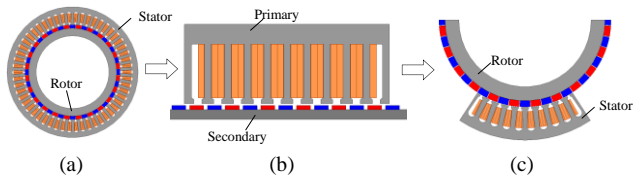


Fig. 2. Evolution process. (a) Rotating motor. (b) Linear motor. (c) PM-ALM.

B. Basic Models

The ALMs can be roughly divided into three different types according to their different topology structures, as shown in Fig. 3. The first type is ALMs with finite length stator and rotor structures, as shown in Fig. 3(a). These ALMs are subject to the circumferential end-effect caused by the finite length of the stator and rotor structures, which are generally used in direct-drive applications with repeated motion within a limited angle, such as wing gate drive system and pitching motor drive system [12]. The second type is ALMs with the finite length stator, as illustrated in Fig. 3(b). This type of motor is generally used in applications where the output

torque is not very high, and only enough torque is required to drive the load motion, such as the azimuth motor drive system of the robot joint [14]. The third type is ALMs having multi-stator modules, and each stator module is of finite length, as shown in Fig. 3(c). This type of ALMs is generally used for special occasions that have certain requirements for the large-sized scanning systems, such as the large telescopes and servo turntable [15].

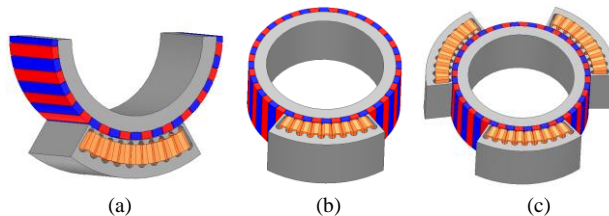


Fig. 3. Three different types of ALMs. (a) Finite arc length stator and rotor structures. (b) Finite arc length stator structure. (c) Multi-stator modules.

III. VARIOUS INDUCTION ALM TOPOLOGIES

In [12], a typical topology of induction ALM is proposed and plotted in Fig. 4. The induction ALM consists of the arc stator and solid rotor. The arc stator structure consists of stator core and armature winding. The motor performance of two induction ALMs having 3-pole double-layer winding and 6-pole single-layer winding are analyzed by the electromagnetic field theory and finite element (FE) method. The results show that compared with the induction ALM with 3-pole double-layer winding, the induction ALM having 6-pole single-layer winding exhibits more symmetry magnetic field. Increasing the number of poles can reduce the degree of mutual asymmetry of the induction ALM. Finally, the analytical and simulation results are validated by the prototype experiment.

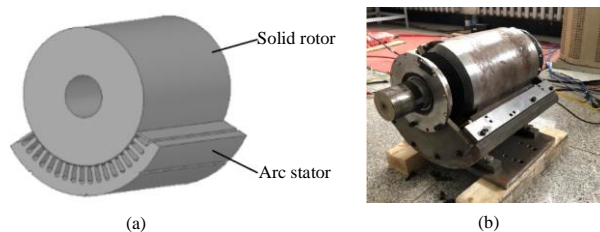


Fig. 4. Illustration of the induction ALM [12]. (a) Topology. (b) Prototype.

In [13], a new electric drive induction arc-linear thruster is designed and used to stretch and shrink the oil tube, as shown in Fig. 5. In the arc-linear thruster, the aluminum sleeve of the oil tube is used as the secondary to reduce the motor volume and weight. In addition, the back iron is added between the aluminum sleeve and oil tube to effectively improve thrust and thrust density.

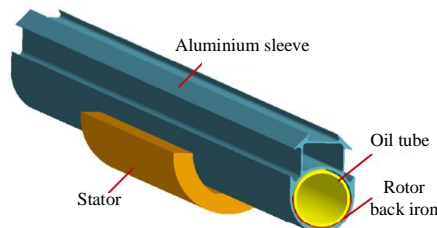


Fig. 5. Topology of the induction arc-linear thruster [13].

In [14]-[15], a single-sided induction ALMs is designed and used to verify the performances of the induction linear motor. The single-sided induction ALM mainly includes primary and secondary parts. As shown in Fig. 6(a), the primary part consists of primary sheet and primary winding. And the secondary part mainly contains secondary sheet and concentric cage. Based on the developed ALM, an experimental platform illustrated in Fig. 6(b) is built, where two coupled induction ALMs with large enough radius are used to simulate the properties of an actual induction linear motor, and to validate the effectiveness of the online identification strategy of secondary time constant and magnetizing inductance [16].

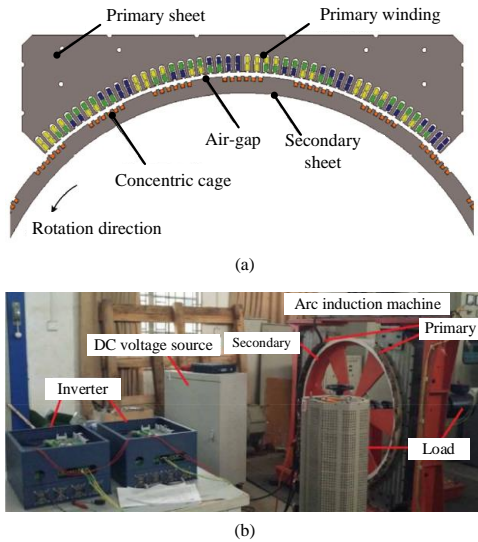


Fig. 6. Single-sided induction ALM [14]-[15]. (a) Topology. (b) Experimental platform.

The proposed ALMs in [12]-[16] can only achieve single-direction (rotation or linear) motion. In order to achieve multi-directional compound motion, a novel two degree-of-freedom (DoF) induction ALM (2DoF-IALM) is proposed in [17], as shown in Fig. 7. The 2DoF-IALM is mainly composed of two arc-shaped stators and a common rotor. Through the interaction of stator and rotor magnetic fields, the 2DoF-IALM can realize rotary, linear, and helical motion. The rotary motion stator and the rotor constitute a rotary motor, and the linear motion stator and the rotor forms a linear motor. The prototype is presented in Fig. 8. Therefore, compared with traditional combined motor, the 2DoF-IALM has the advantages of compact structure and high reliability. To further explore the unique characteristics and performance of the 2DoF-IALM, the helical motion characteristics [18], the 3-D FE and prototype experiment [19], the helical motion coupling effect [20], the stator-slot and pole-pair combinations [21] are comprehensively studied.

In [22], a new 2DoF-IALM with the four circumferential symmetrical arc-shaped stator modules is proposed to weaken the unbalanced radial force. As illustrated in Fig. 9, the stator modules 1 and 2 are circumferential symmetrical in structure and space, which provide linear magnetic fields. The stator modules 3 and 4 are also circumferential symmetrical, which

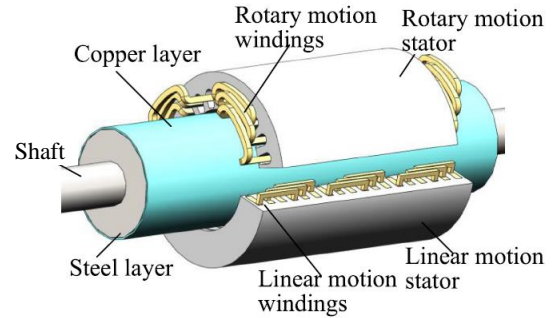


Fig. 7. Topology structure of the 2DoF-IALM [17].

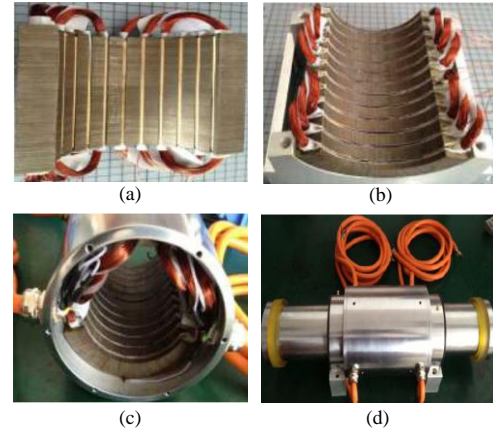


Fig. 8. Prototype of the 2DoF-IALM [17]. (a) Linear motion stator. (b) Rotary motion stator. (c) Whole stator. (d) Whole prototype.

are used to provide rotating magnetic field. Benefiting from the symmetry of the four arc-shaped stators in structure and space, the total radial force of the rotor is effectively cancelled. Hence, this ALM has the advantages of reducing bearing wear, easy control and easy machining and assembly.

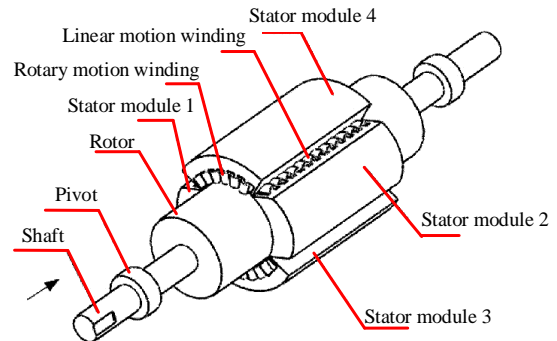


Fig. 9. Topology of the 2DoF-IALM with four circumferential symmetrical arc-shaped stator modules [22].

IV. VARIOUS SYNCHRONOUS ALM TOPOLOGIES

A. Rotor-PM Type ALMs

As a special PM synchronous motor, rotor-PM (RPM) type ALMs have the merits of high efficiency, high torque and fast dynamic response. It is a promising choice for directly driving the large servo systems. According to the different flow path of PM flux, the RPM type ALMs can be subdivided into radial flux-, axial flux- and tubular ALMs.

1) *Radial Flux ALMs*

In [23], a new radial flux ALMs with three arc-shaped stator modules is proposed, as shown in Fig. 10. The authors analyzed the torque fluctuation caused by the asymmetric effect of the three phase armature windings, and put forward a solution of phase-changing connection of stator windings to restrain the torque fluctuation caused by the asymmetric effect of the three phase winding. Besides, in order to further improve the average torque, the authors proposed another ALM with four arc-shaped stator modules in [24], as depicted in Fig. 11. The ALM consists of four stator modules and a hollow cupped rotor. Each stator module is composed of the stator core and the armature winding, and the cupped rotor consists of the rotor core and the parallel magnetized PMs attached to the rotor core. By optimizing the stator length and PM parameters, the torque ripple is reduced to 2%, which satisfies the requirements of the telescope drive.

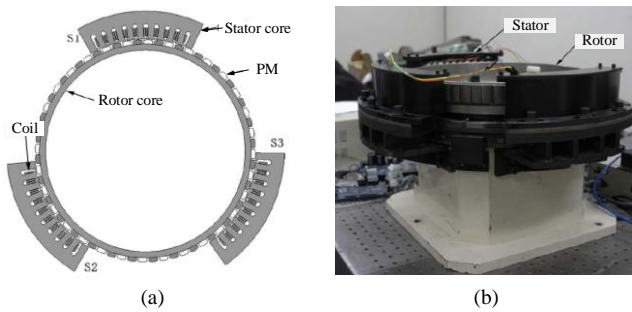


Fig. 10. ALM with three stator modules [23]. (a) Topology. (b) Prototype.

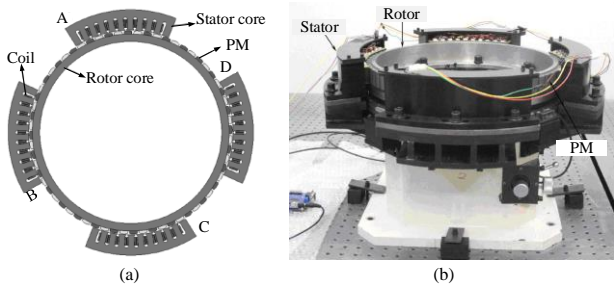


Fig. 11. ALM with four stator modules [24]. (a) Topology. (b) Prototype.

The torque ripple and scanning range of an ALM with unit motor having 9/8 stator-slots/rotor-poles combination used for direct-drive scanning system are investigated in [25]. It shows that after the optimization, the smooth scanning range is greatly increased by 19.5% with a low torque ripple of 3%. [26] studies the influence of the shape of the first and second PMs at the end of the rotor on the torque performance of the ALM. By optimizing the shape of these two PMs, the torque ripple caused by the end-effect is effectively suppressed. In [27]-[28], a new ALM with compensation winding is proposed, as shown in Fig. 12. In order to reduce magnetic resistance and expand the travel range, a set of compensation windings are placed on the end slot of the stator of the ALM. And then, by controlling the DC current in the compensation windings, the magnetic resistance caused by the end-effect is effectively reduced, and the high-precision tracking of the ALM used for the scanning system is ensured. In addition, a winding cross connection method is investigated in [29],

which effectively suppress the torque ripple caused by the end-effect.

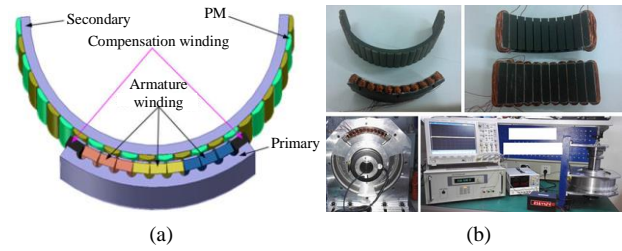


Fig. 12. ALM with compensation winding [28]. (a) Topology. (b) Test platform.

In 2008, a direct-drive Galileo Sphere robot joint used for picking goods is designed in [30]. The direct-drive robot joint is driven by ALMs, which can realize 5DoF motion. As shown in Fig. 13, the pitching ALM is a stator-PM type motor, which can achieve motion range of 106 degree, and the azimuth ALM is a RPM type motor, which can achieve circular motion of 360 degree. The ALMs-based Galileo Sphere robot can carry 4 kg of cargo, and has high control accuracy with 100 μ m.

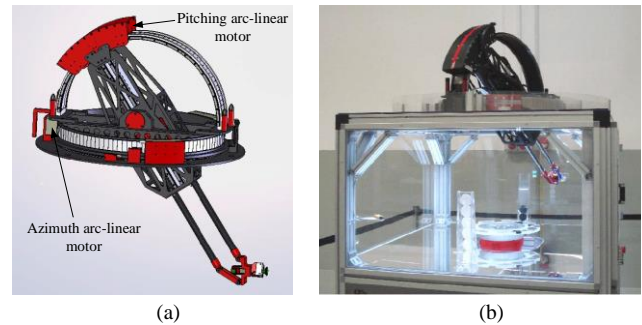


Fig. 13. Galileo Sphere robot joint [30]. (a) Motor topology. (b) Test platform.

2) *Axial Flux ALMs*

Compared with traditional radial flux motor, axial flux motor has higher torque/efficiency density. In [31], the design concept of axial flux motor is introduced into ALM to propose a new single-sided axial flux ALM. The ALM includes the arc-shaped primary segment and linear secondary segment. Therefore, the coupling area between the primary and secondary becomes small, which results in low average thrust and relatively high thrust ripple. In order to further improve the thrust performance, the field analysis and thrust optimization is performed. In addition, a new segmented detent force analytical model is established and investigated. After that, two new optimization methods are proposed to suppress the detent force in [32]-[33]. Finally, the structure of single-sided axial flux ALM shown in Fig. 14 is made as prototype to validate the effectively of the design, as shown in Fig. 15.

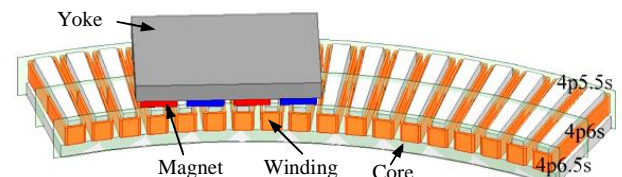


Fig. 14. Structure of single-sided axial flux ALM [32].

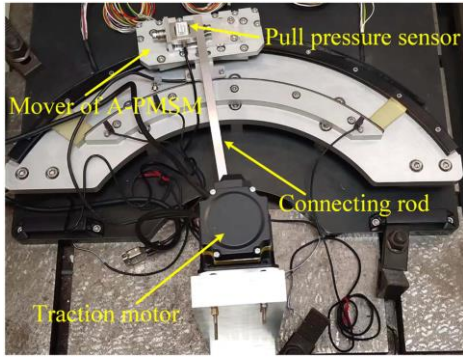


Fig. 15. Prototype of the single-sided axial flux ALM [32].

[34] proposes a double-sided axial flux ALM for driving scanning system, as shown in Fig.16. In order to solve the time-consuming problem caused by 3D FE calculation, an approximate equivalent 2D calculation model is established to calculate the electromagnetic properties of the axial flux ALM. Benefiting from the double-sided structure, the proposed ALM has the advantages of high torque density and low torque ripple. Besides, the double-sided structure can effectively reduce the normal force along the axis.

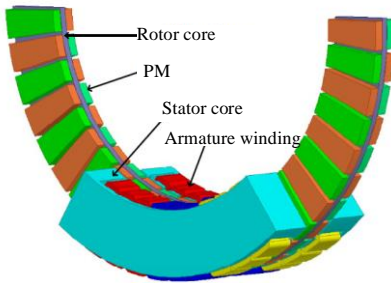


Fig. 16. Topology structure of double-sided axial flux ALM [34].

3) Tubular ALMs

In order to improve the torque density of ALM, a RPM type ALM with 3D air-gap structure is proposed in [35], as shown in Fig. 17(a). The RPM type ALM consists of a rotor structure and four stator segments. The stator core and armature winding form a C-shaped structure. Compared with the ordinary ALM, this ALM shows 1.6 times higher torque density and 47% lower torque fluctuation. In addition, the research group also proposes a Halbach type tubular ALM in [36], as illustrated in Fig. 17(b). The 360 degree full air-gap formed by stator and rotor increases the effective air-gap area involved in energy conversion, which makes the proposed tubular ALM shows higher output torque capacity than the traditional ALM.

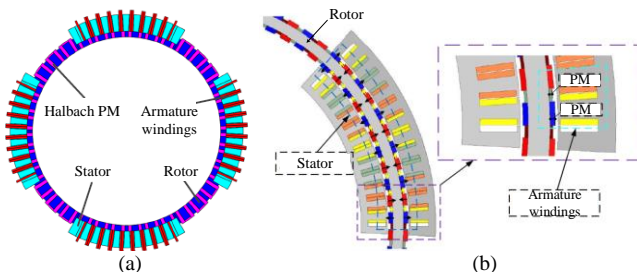


Fig. 17. Topologies of two different ALMs. (a) ALM with 3D air-gap structure [35]. (b) Tubular ALM [36].

In [37], a novel semicircular tubular ALM with trapezoidal PMs is proposed to improve the thrust performances, as shown in Fig. 18. By analyzing magnetic distribution characteristics, it is found that compared with the conventional counterpart, the semicircular tubular ALM with trapezoidal PMs shows superior magnetic flux characteristics. In addition, the mathematical modeling of the semicircular tubular ALM is carried out based on vector potential with Landen's transformation [38]-[39]. The bilateral control of semicircular tubular ALM with disturbance model based on trigonometric function is investigated [40]. The results show that the bilateral control can realize high and stable position tracking.

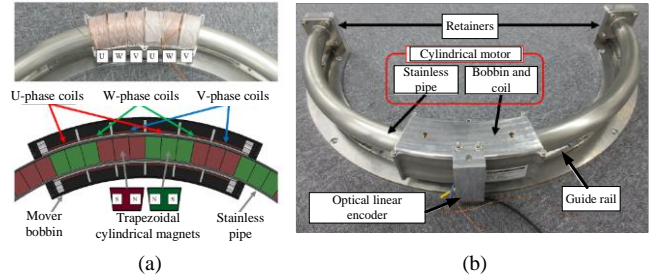


Fig. 18. The semicircular tubular ALM [39]. (a) Topology. (b) Prototype.

B. Stator-PM Type ALMs

For the abovementioned RPM type ALMs, all the PMs are attached to the rotor core along the circumference. However, only a part of effective PMs participate in the torque generation during the operation of ALMs. The remaining PMs are exposed to the air and hence do not participate in the energy conversion. Therefore, RPM type ALMs have the low PM utilization rate. In addition, the RPMs are exposed to air, which can cause safety problems. In order to resolve the problems, the stator-PM (SPM) type ALMs concentrate the PMs on the arc-shaped stator, which can participate in the torque generation, and have become the research hotspot for ALM in recent years. According to the different position of PM, SPM type ALMs are divided into the double salient, FR and FS ALMs.

1) Double Salient ALMs

In this section, the design concept of "double salient (DS) PM motor [41]-[42]" is combined with "partitioned-stator (PS) design [43]-[45]", and introduced into the design field of ALM, and eventually a new DS-ALM is proposed in [46]. Fig. 19 shows the 3D explosion diagram and 2D cross section diagram of the motor, which is mainly composed of three inner stator modules, three outer stator modules and one rotor module sandwiched in the inner and outer stator modules. Tangentially magnetized PMs are placed in the iron core yoke of the inner stator, and the magnetization direction of adjacent PMs is opposite, which constitutes the magnetic agglomeration effect. Benefiting from the magnetic agglomeration effect and PS design, the internal space of the ALM is effectively utilized, which greatly improves the output torque capacity of the entire DS-ALM.

In order to achieve good motor performance of the DS-ALM, a multi-objective optimization method based on

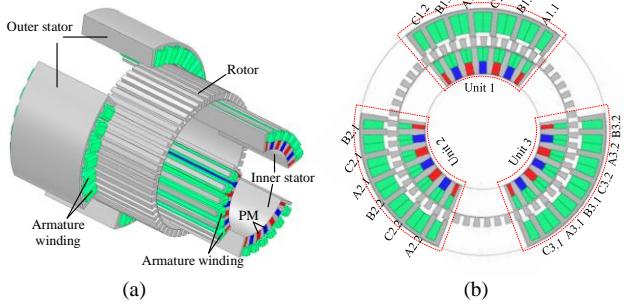


Fig. 19. Topology of the DS-ALM [46]. (a) 3D explosion structure. (b) 2D cross section structure.

LightGBM technique and differential evolution algorithm is proposed in [47]. Finally, the prototype is manufactured shown in Fig. 20 to validate the effectiveness of the above-mentioned optimization design method. In addition, a two-step strategy by combining the cross-winding connection method and machine learning XGBoost-based optimization method is proposed in [48], which well effectively suppress torque fluctuation caused by the asymmetric effect of the three-phase winding.

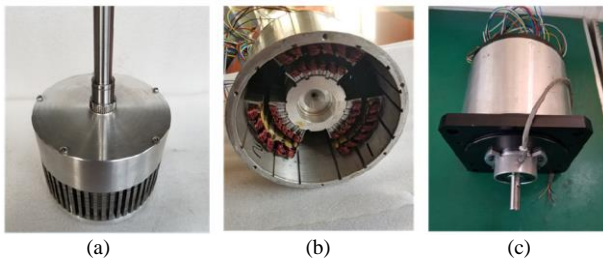


Fig. 20. Motor prototype of the DS-ALM [47]. (a) Salient rotor. (b) Assembled stator. (c) Whole Prototype.

In [49]-[51], a PS hybrid excited (HE) ALM (PS-HE-ALM) is proposed and investigated, as shown in Fig. 21. The PS-HE-ALM can be regarded as the combinations of the ALM, the PS motor and the HE motor. By adjusting the DC field current, the air-gap flux density can be weakened and enhanced flexibly, resulting in good flux adjustment capability, as depicted in Fig. 22. Moreover, benefitting from the PS structure, the space confliction between the magnetic loading and the electrical loading is addressed. Therefore, compared with the traditional single-sided HE-ALM (SS-HE-ALM), the proposed PS-HE-ALM shows improved back-electromotive force (back-EMF) and average torque, as shown in Figs. 23-24. In [52], a new optimization design method by combining random forest method and differential evolution algorithm is investigated to optimize the PS-HE-ALM, which achieve the optimal motor performance.

2) Flux Reversal ALMs

In order to solve the problem of large PM usage in RPM type ALMs, a new FR-ALM (FRALM) is proposed and analyzed by incorporating the concept of “FR motor [53]-[54]” into an ALM. Its topology is shown in Fig. 25. The FRALM consists of three stator modules and a rotor module. The inner diameter of each stator module is affixed with “N-S-iron-S-N-iron” PM and iron core block array, the magnetization direction of PM is radial, and the

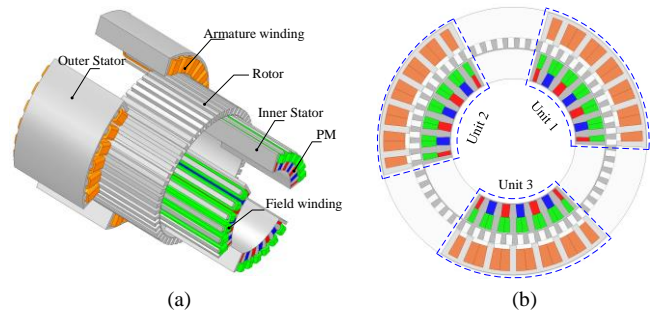


Fig. 21. Topology of the PS-HE-ALM [51]. (a) 3D view. (b) Cross section.

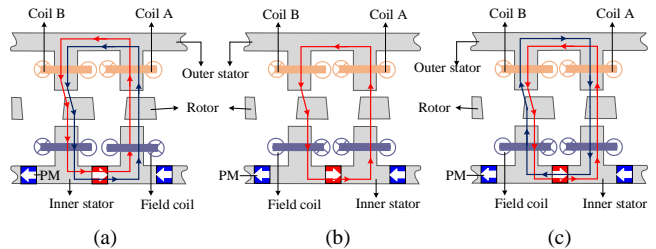


Fig. 22. Working principle of the PS-HE-ALM at three different states [51]. (a) Flux-enhanced state. (b) Only-PM state. (c) Flux-weakened state.

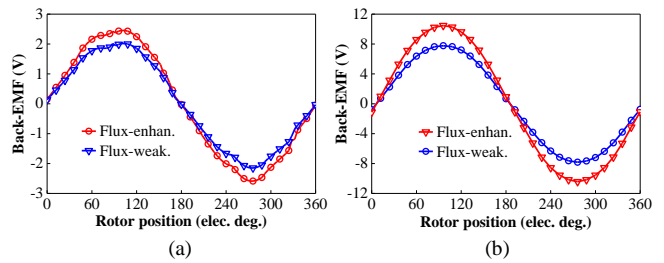


Fig. 23. Comparison of the back-EMF of two ALMs. (a) SS-HE-ALM. (b) PS-HE-ALM.

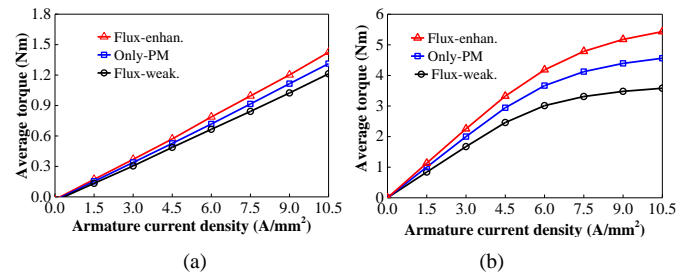


Fig. 24. Comparison of the torque characteristics of two ALMs. (a) SS-HE-ALM. (b) PS-HE-ALM.

magnetization direction of adjacent PMs on each stator tooth is opposite, while the magnetization direction of two PMs on adjacent stator teeth is the same [55]-[56]. It is found that due to the SPM design, all the PMs are effective, which can participate in torque generation and have improved PM utilization rate. In addition, the powerful machine learning algorithm CatBoost is introduced into optimal design field of ALM to obtain optimal structural parameters [57]. Finally, the optimal design method and simulation results are validated by the prototype experiment, as shown in Figs. 26-27.

The previous FRALM depicted in Fig. 25 is a single-sided FRALM, the single-sided structure restricts the further increase of the torque density of the ALM. Therefore, in order to further improve the torque density of ALM, the double-

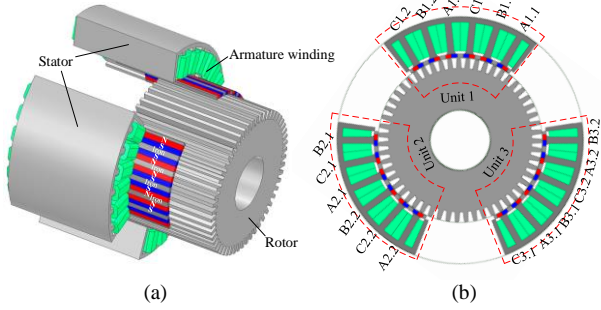


Fig. 25. Topology of the FRALM [57]. (a) Exploded-view. (b) Cross-section.

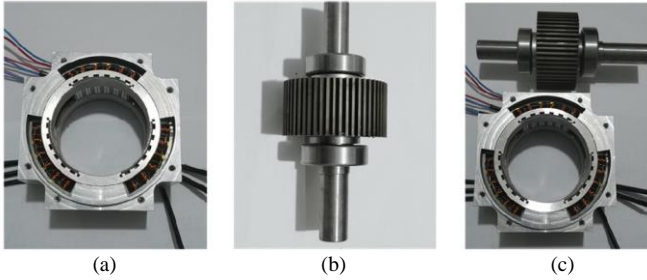


Fig. 26. Prototype of the FRALM [57]. (a) Stator. (b) Rotor. (c) Prototype.

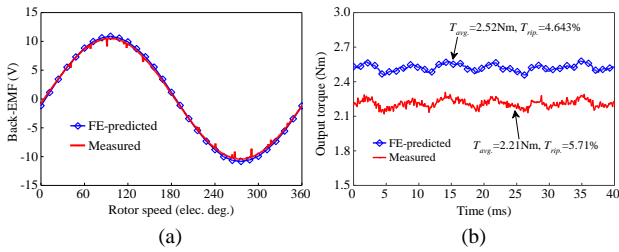


Fig. 27. FE-predicted and measures results. (a) Back-EMF. (b) Output torque. sided structure is introduced into ALM, and eventually a new double-sided FRALM (DS-FRALM) are proposed in [58], as shown in Fig. 28. In this ALM, the inner and outer stator teeth are affixed with radially magnetized SPMs. The magnetization direction of the adjacent PMs on the same tooth is opposite, and the adjacent PMs on the adjacent teeth are in the same direction. Besides, the PM magnetization direction of the inner and outer stators is opposite, so that there is no magnetic coupling between the inner and outer stators. The comparative results shows that the proposed DS-FRALM shows higher average torque compared with the single-sided counterparts.

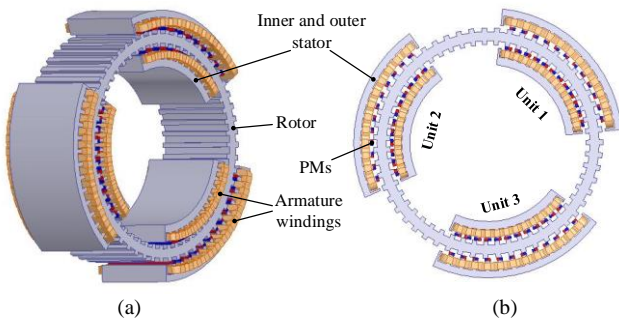


Fig. 28. Topology of DS-FRALM [58]. (a) Exploded-view. (b) Cross-section.

In [59]-[60], the consequent-pole (CP) design is introduced into DS-FRALM to design two CP-DS-FRALMs (named

motor I and motor II, respectively), as shown Fig. 29. It is found that compared to motor II, motor I shows lower cogging torque and better over-load torque capability, but it has lower back-EMF, torque density and PM utilization. The ALMs proposed in [55]-[60] have the relatively constant air-gap PM flux, which lead to limited flux adjustment capability. Consequently, a new HE-DSFRALM as shown in Fig. 30 is proposed by combining the FRALM having double-sided design and the HE motor [61]. The proposed HE-DSFRALM incorporates the merits of high average torque, low cogging torque and wide flux adjustment capability, which is suitable for large telescope drive.

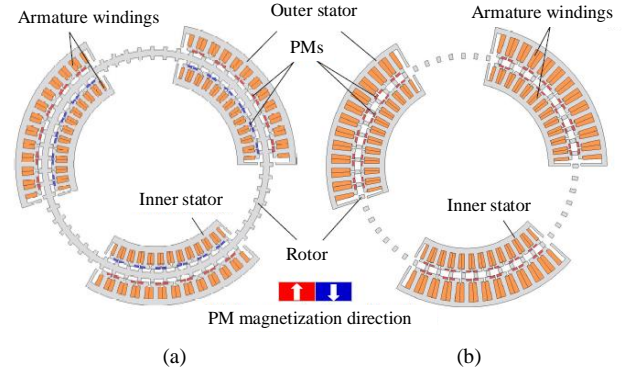


Fig. 29. Two topologies of the CP-DSFRALM [60]. (a) Motor I. (b) Motor II.

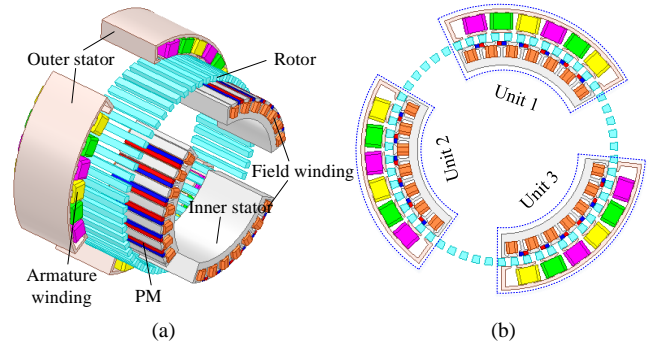


Fig. 30. Topology of the HE-DSFRALM [61]. (a) 3D view. (b) Cross-section.

3) Flux Switching ALMs

In addition to the DS and FR structures, another SPM motor named “FS motor [62]-[64]” is also introduced into the topology design field of ALM to propose three different types of FSALMs in [65]. The first motor is a modular FSALM with three stator modules (named motor I), the second one is the traditional FSALM (named motor II), and the last one is a FSALM having PMs on both stator end-sides (named motor III), as illustrated in Fig. 31. The comparative results show that compared with motors I and III, motor II has better magnetic field distribution, and can output more sinusoidal back-EMF and higher average torque. It is found in [66] that the torque ripple of modular FSALM is mainly caused by the first and second harmonics of cogging torque. In order to reduce the torque ripple, the first harmonic of cogging torque is reduced by optimizing the width of the middle stator module and the left and right ends of the non-magnetic connector. And the second harmonic of cogging torque is reduced by current harmonic injection method. Besides, the

segmented skew rotor pole is adopted to suppress torque pulsation, and comparison results verified the proposed design [67].

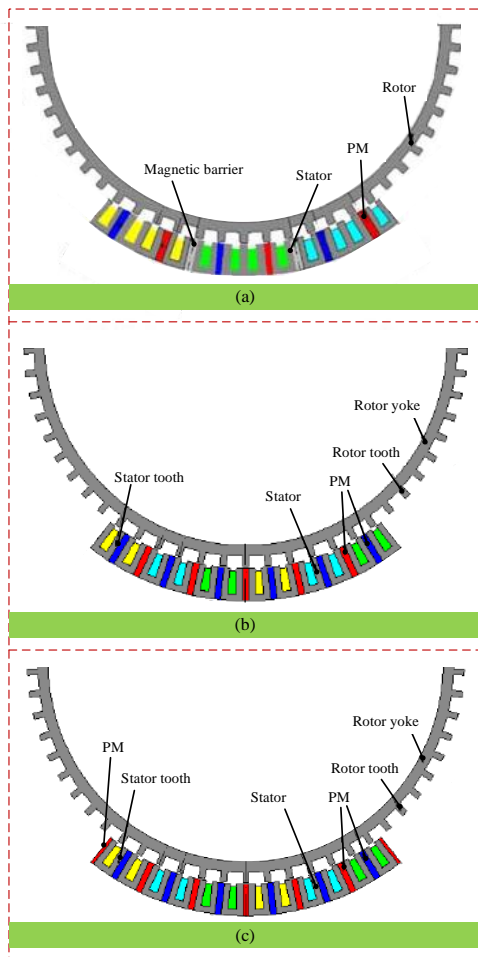


Fig. 31. Three types of FSALMs [65]. (a) Motor I. (b) Motor II. (c) Motor III.

Another new modular FSALM with staggered rotor structure (SR-FSALM) is proposed in [68], as depicted in Fig. 32. The motor adopts a two-stator module with opposite magnetized SPMs. And the SR-FSALM utilizes two staggered rotor to eliminate the even-order harmonics of the back-EMF, thereby reducing the cogging torque and torque ripple.

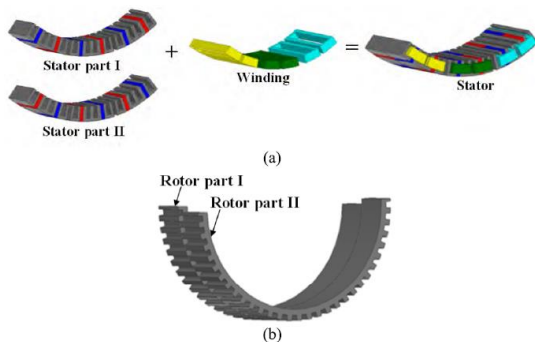


Fig. 32. Topology of SR-FSALM [68]. (a) Stator structure. (b) Rotor structure.

In [69], the basic topology and design principle of FSALM with 6 stator slots /5 rotor teeth are investigated and

discussed. In addition, the analytical models of no load torque and radial force by using magnetic permeance function are established. The derived analytical models show that only pure structural parameter optimization could not achieve the radial force suppression. To effectively suppress the no-load torque and radial force at the same time, a novel double 3-phase FSALM with fault tolerance structure (FT-FSALM) is proposed in [69], as show in Fig. 33. Finally, the simulation and experimental results verify the effectiveness of the proposed design. In [70], on the basis of FT-FSALM, the influence of different winding structures on open circuit fault tolerance currents are analyzed. Then, the performances analysis of fault tolerance under different conditions are carried out from the view of motor temperature rises. Finally, some calculation results show that the FT-FSALM shows improved fault tolerance of open-circuit fault, while having stable heat dissipation and satisfactory average torque output capacity.

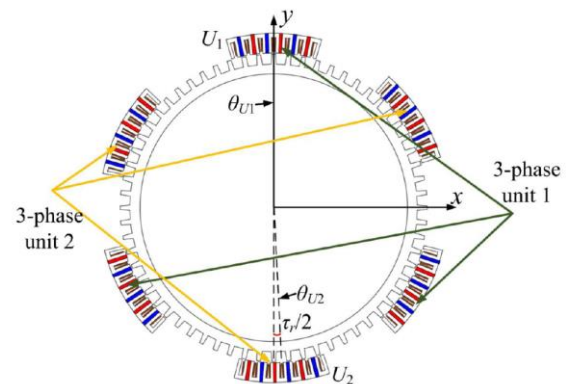


Fig. 33. Motor topology of the double 3-phase FT-FSALM [69].

As shown in Fig. 34, a flux modulated ALM with hybrid PM arrangement (HPM-FMALM) is proposed and analyzed. The proposed HPM-FMALM using hybrid PM arrangements can perform the double flux-modulation effect to improve torque performance [71]. Besides, another new asymmetric dual-stator flux modulated ALM (ADS-FMALM) is proposed in [72]-[73], as illustrated in Fig. 35. The proposed design incorporating the FR structure and FS structure. First, the working principle and optimization design are conducted, and then, the comparative analysis between single- and double-stator configurations is carried out. It is found that the proposed ADS-FMALM shows superior synthetical torque capabilities and is more suitable for direct-driven system applications.

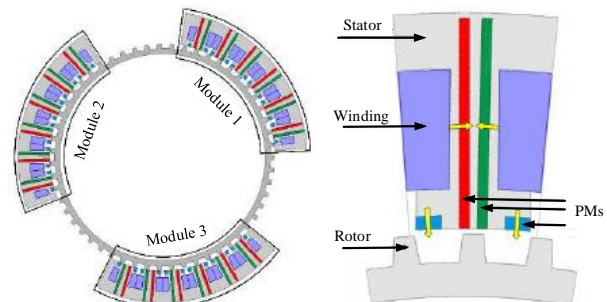


Fig. 34. Motor topology of the HPM-FMALM [71].

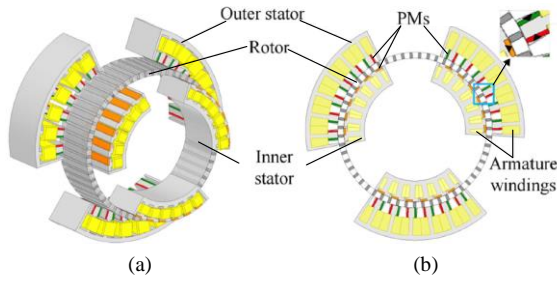


Fig. 35. Motor topology of the proposed ADS-FMALM [72]-[73]. (a) Exploded-view. (b) Cross-section.

C. Dual-PM Type ALMs

The DPM type motors generally refer to a class of motors in which all the PM excitation sources are located in both the stator (primary) and rotor (secondary) structures [74]-[77]. Based on the bidirectional flux modulation effect (BFME), the DPM type motors can enrich the air-gap flux harmonics and effectively improve the torque output capacity of the motor. Therefore, in [78], a new DPM type variable flux ALM (DPM-VFALM) having DPM and DC field winding excitations is developed by combining DPM type motor and ALM structures, as shown in Fig. 36. The flux regulation principle, air-gap field distributions, flux linkage, back-EMF and torque characteristics under different excitation states are analyzed. The results are shown in Fig. 37. It is found that the proposed DPM-VFALM has higher torque characteristics compared with SPM- and RPM counterparts.

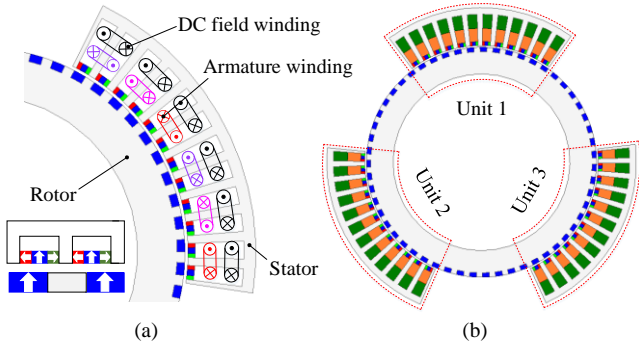


Fig. 36. Topology of DPM-VFALM [78]. (a) One module. (b) Whole motor.

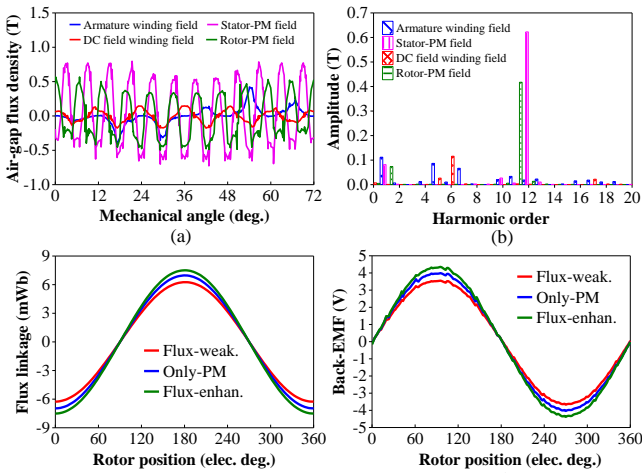


Fig. 37. Flux regulation principle of the DPM-VFALM. (a) Field distributions. (b) Harmonic analysis. (c) Flux linkage. (d) Back-EMF.

As illustrated in Fig. 38, a new multi-unit distributed DPM excited ALM (DPM-ALM) is proposed [79]-[80]. Comparative results indicate that the proposed DPM-ALM exhibits improved output torque capability benefiting from the BFME. In addition, the CP design is also introduced into the proposed DPM-ALM, which make the DPM-ALM show higher PM utilization rate compared with the RPM type and middle SPM (MSPM) type counterparts. Finally, the simulation results are validated by the prototype experiment depicted in Fig. 39. The finite element results and experimental results are illustrated in Fig. 40.

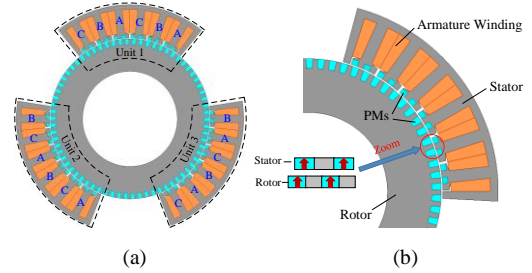


Fig. 38. Topology of the DPM-ALM [80]. (a) Whole motor. (b) Unit motor.

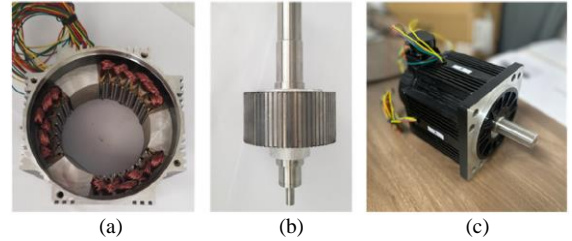


Fig. 39. Prototype of the DPM-ALM [80]. (a) Stator. (b) Rotor. (c) Prototype.

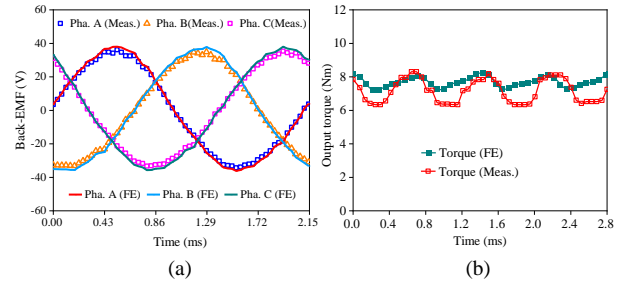


Fig. 40. Comparison of measured and FE results. (a) Back-EMF. (b) Torque.

D. Performance Comparison

Through the summary of the above investigations in Sections III and IV, it can be found that different types of ALMs have advantages and disadvantages. Firstly, the merits and demerits of four types of ALMs (i.e., Induction ALMs, RPM type ALMs, SPM type ALMs and DPM type ALMs) are summarized. Then, the electromagnetic performances of several typical PM ALMs are compared in Table I.

The analysis is summarized as follows:

1) For the induction ALMs: induction ALM is asynchronous motor, its torque fluctuation is relatively high compared with PM-ALMs. In addition, the rotor of the induction ALMs is generally a solid and simple structure. However, the solid rotor produces eddy current loss, which could result in relatively high temperature rise and low power factor.

2) For the RPM type ALMs: compared with the SPM type

ALMs, the RPM type ALMs are easier to manufacture and have relatively higher reliability. However, only part of RPMs is involved in the torque generation, while the remaining PMs are exposed to the air and does not participate in the torque generation, which has relatively low PM utilization rate, high PM usage and failure rate.

3) For SPM type ALMs: compared with the RPM type ALMs with surface-mounted PM (SMPM) arrangement, the SPM type ALMs have relatively lower torque. However, the SPM type ALMs fully and effectively utilize all the SPMs for torque generation, resulting in a relatively high PM utilization rate and low PM cost, as listed in Table I.

4) As for DPM type ALMs: although PMs are wrapped in stator and rotor core, which results in high PM usage and cost, the BFME is an effective solution to heighten the torque capacity of ALM under the limited space constraints. Currently, it has gradually attracted increasing attention.

V. ADVANCED CONTROL TECHNIQUES

Because of its unique finite length structure, the ALM will also be affected by some periodic and aperiodic disturbances, which will make motor speed fluctuate obviously at low speed. Therefore, it is of great significance to find a suitable control algorithm to improve position and speed tracking performance of the whole ALM control system.

In [81], a new model predictive control (MPC) based on extended state observer (ESO) and iterative learning control (ILC) is designed and shown in Fig. 41. The ESO is fed forward to the MPC controller to reject the nonperiodic slowly changing disturbances. Then, the ILC is used to compensate the periodic position-dependent disturbances. Finally, the experimental results show that the proposed control system has better speed tracking and speed disturbance rejection ability.

TABLE I
MAIN STRUCTURAL PARAMETERS AND PERFORMANCE COMPARISON OF SEVERAL TYPICAL ALMS

Parameters	SMPM-ALM	DS-ALM	Inner rotor-ALM	Outer rotor-ALM	DS-FRALM	RPM-ALM	SPM-ALM	DPM-ALM	MSPM-ALM
Reference	[46]	[46]	[46]	[46]	[58]	[80]	[80]	[80]	[80]
Motor outer radius/mm	68	68	68	68	68	61	61	61	61
Motor inner radius/mm	32	32	32	32	32	15	15	15	15
Stator slot numbers of each Unit	6	6	6	6	6	6	6	6	6
Rotor pole numbers of each Unit	11	11	11	11	11	14	14	14	14
Stack length/mm	50	50	50	50	50	40	40	40	40
Air-gap length/mm	0.55	0.55	0.55	0.55	0.55	0.5	0.5	0.5	0.5
Stator tooth pitch (degree)	12.0	12.0	12.0	12.0	12.0	12.0	12.0	12.0	12.0
Rotor pole pitch (degree)	72/11	72/11	72/11	72/11	72/11	72/14	72/14	72/14	72/14
Rotor outer arc ratio	–	0.5	0.3	0.5	0.6	0.47	0.47	0.47	0.47
Rotor outer arc ratio	–	0.3	0.6	0.3	0.5	0.6	0.6	0.6	0.6
SPM height/mm	–	7.12	6.4	6.7	1.5	–	1.6	1.6	1.6
RPM height/mm	2.0	–	–	–	–	1.98	–	1.98	1.98
Rotor teeth height/mm	–	5.11	5.5	4.5	1.375	1.98	1.98	1.98	1.98
PM grade	N42SH	N42SH	N42SH	N42SH	N42SH	N42SH	N42SH	N42SH	N42SH
Silicon steel grade	DW310-35	DW310-35	DW310-35	DW310-35	DW310-35	DW310-35	DW310-35	DW310-35	DW310-35
Maximum back-EMF (V)	11.4	10.46	5.40	9.45	9.74	19.75	13.22	36.91	14.38
Average torque/(N m)	3.97	3.49	1.85	2.86	3.42	4.55	3.24	7.70	2.78
Peak to peak torque/(N m)	0.704	0.046	0.312	0.168	0.501	1.61	1.16	0.94	0.99
Total PM usage/(cm ³)	31.9	23.58	24.5	18.9	19.8	10.11	3.83	13.94	13.94
Torque/total PM usage/(N m/cm ³)	0.12	0.148	0.076	0.151	0.173	0.450	0.846	0.552	0.199

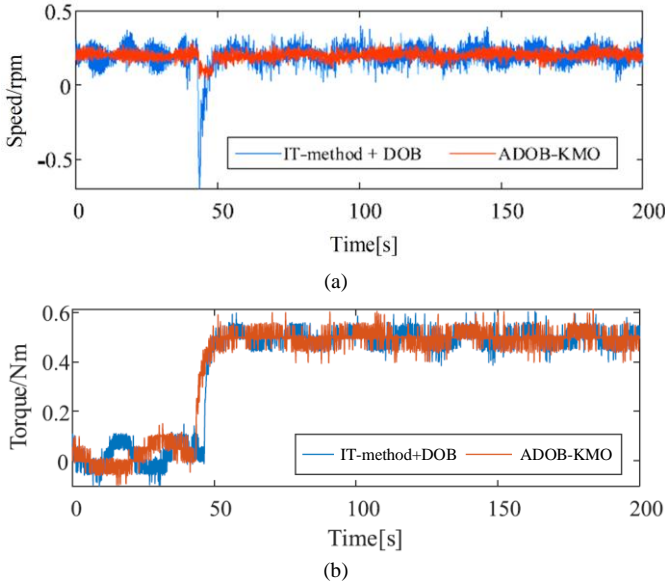


Fig. 46. Experimental results of speed and torque tracking based on two different control methods [85]. (a) Speed waveform. (b) Torque waveform.

The ALM offer suffers from the speed ripple due to the periodic disturbances. The traditional disturbance observer can reduce the speed ripple by increasing the observer bandwidth, but this will introduce high-frequency noise. In order to address the limitations, a new high-pass filter-based linear active disturbance rejection controller (HFLADRC) shown in Fig. 47 is proposed to drive the ALM in [86]. The experimental results of PI and HFLADRC control methods at 10 r/min are compared in Fig. 48. It can be seen that in the two control methods, the PI control method has the worst speed tracking capability. This is because that the peak-peak value of speed ripple is the biggest. However, the peak-peak value of speed ripple of the HFLADRC is the smallest, which indicates that the proposed HFLADRC method is more capable of effectively suppressing speed ripple.

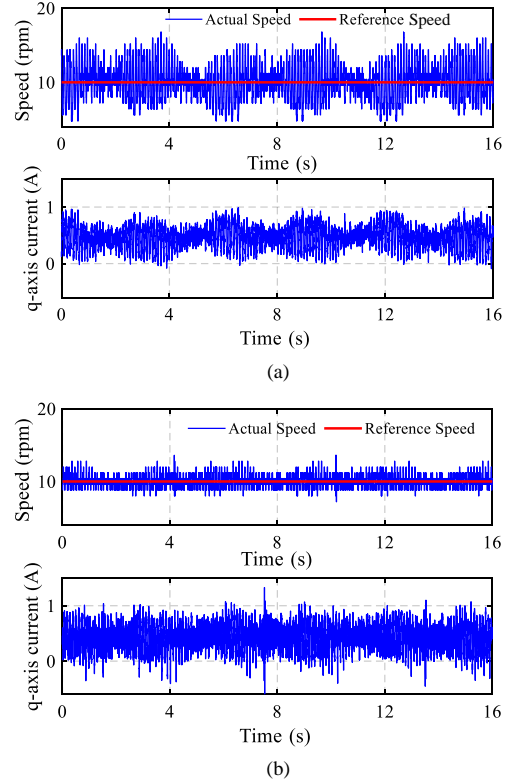


Fig. 48. Experimental results of two control methods at 10r/min [86]. (a) PI. (b) HFLADRC.

developed [8]-[9]. Since then, the ALMs have been widely applied on some famous large telescopes including the TMT [8], Subaru [10] and ALMA [11], and so on [23]-[29]. Different from the traditional solution of rotating PM motor plus gearboxes, ALMs directly connect load without auxiliary devices. Thus, compared with the traditional solution, the response performance and the drive efficiency of the transmission system based on the ALMs are greatly improved. In addition, ALMs can be manufactured piecewise and assembled on site, which effectively reduce the machining cost. Therefore, ALMs have been regarded as good candidate for large telescope drive, especially the DPM type ALMs [78]-[80].

2) Robot Joint Systems

Through pre-research, it can be found that the remarkable characteristics of multi-DoF robots such as palletizing robots and medical robots in the operation process are as follows: The motion trajectory planned by multi-DoF robots is often not a complete rotation motion, but frequent and repeated motion in a limited Angle and high-precision positioning. To realize the multi-DoF limited angular motion, the traditional solution is rotating PM motor plus gear box, where the rotating motion can be converted to linear motion. However, the additional gear box will introduce the transmission error and complex mechanical structure. Direct-drive motor can avoid the above-mentioned limitations. The ALMs have the dual characteristics of rotating PM motor and linear PM motor, which have the features of fast dynamic response and direct-drive characteristics [87]. Besides, the stator or rotor of the ALMs is finite length structure, which is consistent with

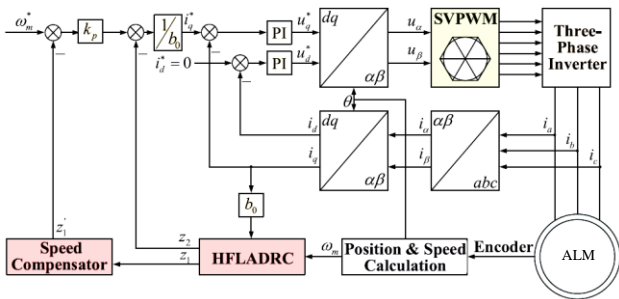


Fig. 47. Block diagram of the control system based on HFLADRC [86].

VI. APPLICATION AREAS AND DEVELOPMENT TRENDS

A. Application Areas

1) Large Telescope Scanning Equipment

The ALM was first introduced in the large telescope drive [9]. With the development of science and technology, the optical telescope becomes larger and larger, the ordinary rotary motors cannot meet the required size for the large telescope [5]-[7]. At the beginning of the 21st century, a new driving system for the large telescope based on the ALM was

the features of the robot motion trajectory. Thus, the “multi-unit modular ALMs” formed by the flexible combination of one or more stator/rotor elements can well realize the limited angular and repeated “zero-motion” of the multi-DoF robots in the process of pitching and horizontal motion. Therefore, due to its unique structural characteristics, under the limited space constraint, the ALM exhibits a good application prospect in direct-drive robot joint applications such as palletizing robots [30] and surgery robots [37]-[40].

3) *Other Electromagnetic Driven Systems*

Servo control systems play an important role in the field of manufacturing and industrial production. The traditional servo control system adopts the indirect form of “rotating motor plus auxiliary mechanism”, which results in the complicated transmission structure, large volume and high manufacturing cost. Besides, the system has defects such as friction and wear, elastic deformation and reverse clearance, which is difficult to meet the requirements of low speed, high torque and high precision. Therefore, direct-drive LAMs have wide application prospects in various servo control systems such as annular transmission system [31]-[33] and servo turntable [23]-[24], [55]-[57], [58]-[61], [78]-[80]. For example, the annular transmission system in [31]-[33] is mainly made up of linear motor and ALM. Moreover, the studied ALM is an axial flux ALM. Compared with radial flux ALM, the axial flux ALM shows higher torque density. In the servo turntable application, various SPM- and DPM type ALMs are designed and thoroughly analyzed in [23]-[24], [55]-[57], [58]-[61], [78]-[80]. Comparative results show that the SPM- and DPM type ALMs have higher PM utilization rate and torque characteristics than the RPM type ALMs. Of course, in addition to the above three typical application areas, direct-drive ALM is also a attractive candidate for other applications including wing gates, drilling machines, biopsies, etc. [17]-[22].

B. *Development Trends*

1) *Main Challenges*

Following the overview on recent ALM technologies, the characteristics of the ALMs are analyzed, and then two main issues can be summarized as follows: (a) The stator or rotor structure of the ALMs is discontinuous along the circumference. Therefore, the finite length structure leads to a reduction in the effective area of the coupling between the stator and the rotor, thus the electromagnetic torque and torque density generated by ALM are relatively lower compared with the traditional rotating PM motor. (b) Similar to ordinary linear PM motors, the ALMs will suffer from the circumferential end-effect due to the finite length of stator or rotor core. Accordingly, in addition to the slotting torque, the circumferential end-effect will generate the additional ending torque and radial force. On the other hand, another effect of the circumferential end-effect is to produce three-phase winding asymmetry effect, resulting in a high load torque fluctuations. Accordingly, based on the above analysis, the ALMs show higher torque fluctuations than the rotating PM motor. Therefore, for the ALM topologies in the future direct-drive applications, the core challenges to be solved are: How

to improve the torque density and reduce the torque ripple of the ALMs under the constraint of limited space volume.

2) *Future Trends*

Focusing on the core challenges of “torque density increase and torque ripple decrease” of the ALMs, this paper intends to summarize the following three future trends from the motor design and control strategy level:

1) Novel ALM topologies will continue to emerge, which attempt to improve torque density and reduce torque fluctuation. The axial flux ALMs and DPM type ALMs seem to be more suitable for direct-drive applications due to its higher torque density than its single PM-counterparts. At present, there are few researches on these two types of ALM designs.

2) Workable data-driven surrogate model-based optimization design methods having high precision and good generalization ability as well as considering the electromagnetic, thermal and mechanical multiphysics are highly required to facilitate the optimization design process of ALMs.

3) Previous research on ALM mainly focuses on improving average torque and reducing torque fluctuation. However, the inherent structural characteristics of the ALM lead to large radial force and temperature rise. Therefore, effective approach to suppress the radial force and temperature rise is still a major challenge for ALM in the future direct-drive applications.

4) Past works on control algorithms for the ALM focus on improving the tracking accuracy and disturbance suppression ability. However, dynamic response ability is also an important performance index of the ALM drive system. The exploration of the advanced control strategies to improve dynamic response performance of the drive system are still highly essential.

VII. CONCLUSION

This paper provides a comprehensive overview of the ALMs for direct-drive applications, mainly focusing on their topology structures, working principles, performances evaluation, and optimization and control techniques. According to the working principle, the ALMs can be classified into two categories, i.e., induction and synchronous ALMs. Further, the synchronous ALMs are classified into RPM, SPM and DPM ALMs. The RPM-ALMs include radial flux, axial flux and tubular ALMs. The SPM-ALMs are divided into double salient, FR and flux switching ALMs. Then, the major merits and demerits of various ALM topologies are identified and summarized. The RPM type ALMs illustrate high torque capability. However, the PM utilization rate is relatively low. On the contrary, the SPM type ALMs can improve PM utilization rate, but the average torque is lower than the RPM type counterparts. The DPM type ALMs can be regarded as a combination of RPM and SPM type ALMs, thus are tradeoffs between the RPM and SPM ALMs. Benefitting from their corresponding features, the ALMs have been widely used in various application areas including the large telescopes, robot joints, servo control

systems, and so on. Finally, we discussed the main issues and core challenges of ALMs, and proposed the perspectives as well to promote a more comprehensive understanding for ALM.

REFERENCES

- [1] M. Y. Jiang, S. X. Niu, and C. C. Chan, "A High-order-harmonic Compound-rotor Based Brushless Doubly-fed Machine for Variable Speed Constant Frequency Wind Power Generation," *IEEE J. of Emerg. and Sel. Topics in Power Electron.*, vol. 13, no. 3, pp. 1492–1502, Apr. 2025.
- [2] Y. M. Shen, Q. F. Lu, and Y. X. Li, "Design Criterion and Analysis of Hybrid-excited Vernier Reluctance Linear Machine with Slot Halbach PM Arrays," *IEEE Trans. on Ind. Electron.*, vol. 70, no. 5, pp. 5074–5084, May 2023.
- [3] K. K. Guo, Y. G. Guo, and S. H. Fang *et al.*, "Design and Analysis of a Permanent Magnet Frameless Motor," *IEEE J. of Emerg. and Sel. Topics in Power Electron.*, vol. 12, no. 3, pp. 3124–3134, Jun. 2024.
- [4] C. M. Martinez, X. S. Hu, and D. P. Cao *et al.*, "Energy Management in Plug-in Hybrid Electric Vehicles: Recent Progress and a Connected Vehicles Perspective," *IEEE Trans. on Veh. Technol.*, vol. 66, no. 6, pp. 4534–4549, Jun. 2017.
- [5] I. Boldea, L. N. Tutelea, and A. A. Popa, "Claw Pole Synchronous Motors/Generators (CP-SMs/Gs) Design and Control: Recent Progress," *IEEE J. of Emerg. and Sel. Topics in Power Electron.*, vol. 10, no. 4, pp. 4556–4564, Aug. 2022.
- [6] Y. T. Gao, M. Doppelbauer, and J. Ou *et al.*, "Design of a Double-side Flux Modulation Permanent Magnet Machine for Servo Application," *IEEE J. of Emerg. and Sel. Topics in Power Electron.*, vol. 10, no. 2, pp. 1671–1682, Apr. 2022.
- [7] Y. Z. Zhang, D. W. Li, and P. Yan *et al.*, "A High Torque Density Claw-pole Permanent-magnets Vernier Machine," *IEEE J. of Emerg. and Sel. Topics in Power Electron.*, vol. 10, no. 2, pp. 1756–1765, Apr. 2022.
- [8] G. Gilardi, K. Szeto, and S. Huard *et al.*, "Finite Element Analysis of the Cogging Force in the Linear Synchronous Motor Array for the Thirty Meter Telescope," *Mechatronics*, vol. 12, no. 3, pp. 116–124, Feb. 2011.
- [9] F. Leonardi, M. Venturini, and A. Vismara, "PM Motors for Direct Driving Optical Telescope," *IEEE Ind. Appl. Mag.*, vol. 2, no. 4, pp. 10–16, Jul. 1996.
- [10] S. Negishi, T. Kanzawa, and D. Tomono *et al.*, "Subaru Telescope Improved Pointing Accuracy in Open-loop and Az Rail Flatness," in *Proc. of SPIE - The International Society for Optical Engineering 6267*, vol. 6267, pp. 1–10, Jun. 2006.
- [11] L. Giacomel, C. Manfrin, and G. Marchiori, "The European ALMA Production Antennas: New Drive Applications for Better Performances and Low Cost Management," in *Proc. of SPIE - The International Society for Optical Engineering*, vol. 7018, pp. 701236, Jun. 2008.
- [12] W. X. Liu, Z. Z. Cui, and W. Hao *et al.*, "Effect of Static Longitudinal End Effect on Performance of Arc Linear Induction Motor," in *Proc. of 2019 22nd Int. Conf. on Electr. Mach. Syst. (ICEMS)*, Harbin, China, Aug. 2019, pp. 1–6.
- [13] C. Feng, Y. L. Bi, and P. X. Liang *et al.*, "Design of Linear Thruster with a Solid Arc-shaped Mover Used by Tanker Aircraft," in *Proc. of 2014 17th Int. Symp. on Electromagn. Launch Technol.*, La Jolla, CA, USA, Jul. 2014, pp. 1–6.
- [14] W. Xu, G. Y. Sun, and G. L. Wen *et al.*, "Equivalent Circuit Derivation and Performance Analysis of a Single-sided Linear Induction Motor based on the Winding Function Theory," *IEEE Trans. on Veh. Technol.*, vol. 61, no. 4, pp. 1515–1525, May. 2012.
- [15] W. Xu, J. Zhu, and Y. C. Zhang *et al.*, "An Improved Equivalent Circuit Model of a Single-sided Linear Induction Motor," *IEEE Trans. on Veh. Technol.*, vol. 59, no. 5, pp. 2277–2289, Jun. 2010.
- [16] D. H. Dong, W. Xu, and X. Y. Xiao *et al.*, "Online Identification Strategy of Secondary Time Constant and Magnetizing Inductance for Linear Induction Motors," *IEEE Trans. on Power Electron.*, vol. 37, no. 10, pp. 12450–12462, Oct. 2022.
- [17] J. K. Si, H. C. Feng, and L. W. Ai *et al.*, "Design and Analysis of a 2-DOF Split-stator Induction Motor," *IEEE Trans. on Energy Convers.*, vol. 30, no. 3, pp. 1200–1208, Sept. 2015.
- [18] L. J. Xie, J. K. Si, and Y. H. Hu *et al.*, "Helical Motion Analysis of the 2-degree-of-freedom Split-stator Induction Motor," *IEEE Trans. on Magn.*, vol. 55, no. 6, pp. 1–5, Jun. 2019.
- [19] L. J. Xie, J. K. Si, and Y. H. Hu *et al.*, "Characteristics Analysis of the Motions of the Two-degree-of-freedom Direct Drive Induction Motor," *IEEE Trans. on Ind. Electron.*, vol. 67, no. 2, pp. 931–941, Feb. 2020.
- [20] L. J. Xie, J. K. Si, and T. F. Wu *et al.*, "Analysis and Suppression Techniques of Helical Motion Coupling Effect for the 2DoF Direct Drive Induction Machine," *IEEE Trans. on Ind. Electron.*, vol. 69, no. 2, pp. 1200–1210, Feb. 2022.
- [21] P. Su, L. J. Xie, and J. K. Si, "Analysis of Stator-slot and Pole-pair Combinations in a Two-degree-of-freedom Split-stator Induction Machine based on Motion Coupling Model," *IEEE Trans. on Ind. Electron.*, vol. 70, no. 12, pp. 12145–12154, Dec. 2023.
- [22] A Two Degree of Freedom Induction Motor, by L.W. Ai. (2014, Jun. 25) CN 203674931U [Online]. Available: <http://epub.cnipa.gov.cn/Sw/SwDetail>.
- [23] J. J. Chang, W. L. Ma, and Y. K. Fan *et al.*, "New Methods for Arc Permanent Magnet Linear Synchronous Motor to Decrease Torque Ripple," *IEEE Trans. on Magn.*, vol. 48, no. 10, pp. 2659–2663, Oct. 2012.
- [24] J. J. Chang, W. L. Ma, and J. L. Huang *et al.*, "Design and Optimization of Arc Permanent Magnet Synchronous Motor Used on Large Telescope," *IEEE Trans. on Magn.*, vol. 48, no. 5, pp. 1943–1947, May 2012.
- [25] H. Z. Hu, J. Zhao, and X. D. Liu *et al.*, "Research on the Torque Ripple and Scanning Range of an Arc-structure PMSM Used for Scanning System," *IEEE Trans. on Magn.*, vol. 50, no. 11, pp. 1–4, Nov. 2014.
- [26] J. Zhao, H. Z. Hu, and X. D. Liu *et al.*, "Influence of Edge Permanent-magnet Shape on the Performance of an Arc-linear Permanent-magnet Synchronous Machine," *IEEE Trans. on Magn.*, vol. 51, no. 11, pp. 1–4, Nov. 2015.
- [27] Z. Chen, H. Zhao, and J. Zhao *et al.*, "Control System and Simulation of Arc-linear Permanent-magnet Synchronous Machine with Compensation Windings," in *Proc. of 2017 20th Int. Conf. on Electr. Mach. and Syst. (ICEMS)*, Sydney, NSW, Australia, Aug. 2017, pp. 1–6.
- [28] B. Li, J. Zhao, and X. D. Liu *et al.*, "Detent Force Reduction of an Arc-linear Permanent-magnet Synchronous Motor by Using Compensation Windings," *IEEE Trans. on Ind. Electron.*, vol. 64, no. 4, pp. 3001–3011, Apr. 2017.
- [29] Z. B. Pan, S. H. Fang, and H. Y. Lin *et al.*, "Torque Ripple Suppression of Arc Permanent Magnet Synchronous Machine based on Winding Cross Connection Method," in *Proc. of 2018 IEEE Int. Conf. on Appl. Supercond. and Electromagn. Devices (ASEMD)*, Tianjin, China, Apr. 2018, pp. 1–2.
- [30] C. Bianchini, F. Immovilli, and A. Bellini *et al.*, "Arc Linear Motors for Direct Drive Robots: Galileo Sphere," in *Proc. of 2008 IEEE Industry Applications Society Annual Meeting*, Edmonton, AB, Canada, Sept. 2008, pp. 1–7.
- [31] Y. S. Liu, and X. Z. Huang, "Suppression of Detent Torque for Arc Permanent Magnet Synchronous Motor based on Variable-height Tooth," in *Proc. of 2023 26th Int. Conf. on Electr. Mach. and Syst. (ICEMS)*, Zhuhai, China, Nov. 2023, pp. 3948–3952.
- [32] Y. S. Liu, X. Z. Huang, and Z. Wang *et al.*, "Analysis and Suppression of Detent Force of Arc Permanent Magnet Synchronous Motor with Linear Mover," *IEEE Trans. on Ind. Electron.*, vol. 71, no. 9, pp. 11167–11175, Sept. 2024.
- [33] Y. S. Liu, X. Z. Huang, and J. Li *et al.*, "Magnetic Field Analysis and Thrust Optimization of Arc Permanent Magnet Synchronous Motor Combined with Linear Mover and Arc Stator," *IEEE Trans. on Ind. Appl.*, vol. 59, no. 5, pp. 5867–5874, Sept.–Oct. 2023.
- [34] J. Zhao, C. C. Zhu, and B. Li *et al.*, "Investigation on an Arc-linear Axial Flux Permanent-magnet Synchronous Machine," in *Proc. of 2017 20th Int. Conf. on Electr. Mach. and Syst. (ICEMS)*, Sydney, NSW, Australia, Aug. 2017, pp. 1–6.
- [35] H. T. Wang, S. H. Fang, and B. C. Guo *et al.*, "A New Halbach Arc Permanent Magnet Synchronous Motor with Three-dimensions Air Gap Used on Large Telescope," in *Proc. of IEEE Int. Conf. on Appl. Supercond. and Electromagn. Devices (ASEMD)*, Shanghai, China, Nov. 2015, pp.1–2.
- [36] S. H. Fang, S. H. Xue, and Z. B. Pan *et al.*, "Torque Ripple Optimization

- of a Novel Cylindrical Arc Permanent Magnet Synchronous Motor Used in a Large Telescope,” *Energies*, vol. 12, no. 3, pp. 362, Jan. 2019.
- [37] M. Omura, T. Shimono, and Y. Fujimoto, “Thrust Characteristics Improvement of a Circular Shaft Motor for Direct-drive Applications,” *IEEE Trans. on Ind. Appl.*, vol. 51, no. 5, pp. 3647–3655, Sept.–Oct. 2015.
- [38] H. Asai, T. Shimono, and Y. Fujimoto *et al.*, “Mathematical Modeling and Analysis of Semicircular Linear Motor,” in *Proc. of 2016 XXII Int. Conf. on Elect. Mach. (ICEM)*, Lausanne, Switzerland, Sept. 2016, pp. 1868–1874.
- [39] H. Asai, T. Shimono, and Y. Fujimoto *et al.*, “Mathematical Modeling of Semicircular Linear Motor based on Vector Potential with Landen’s Transformation,” *IEEE Trans. on Ind. Appl.*, vol. 55, no. 1, pp. 437–447, Jan.–Feb. 2019.
- [40] H. Asai, M. Omura, and T. Shimono *et al.*, “Bilateral Control of a Half-circle-shaped Tubular Linear Motor with Disturbance Model based on Trigonometric Function of Two Variables,” in *Proc. of 7th International Conference on Information and Automation for Sustainability*, Colombo, Sri Lanka, Dec. 2014, pp. 1–6.
- [41] Y. F. Liao, F. Liang, and T. A. Lipo, “A Novel Permanent Magnet Motor with Doubly Salient Structure,” *IEEE Trans. on Ind. Appl.*, vol. 31, no. 5, pp. 1069–1078, Sept.–Oct. 1995.
- [42] T. T. Sheng, S. X. Niu, and S. Y. Yang, “A Novel Design Method for the Electrical Machines with Biased DC Excitation Flux Linkage,” *IEEE Trans. on Magn.*, vol. 53, no. 6, pp. 1–4, Jun. 2017.
- [43] D. J. Evans, and Z. Q. Zhu, “Novel Partitioned Stator Switched Flux Permanent Magnet Machines,” *IEEE Trans. on Magn.*, vol. 51, no. 1, pp. 1–14, Jan. 2015.
- [44] Q. F. Lu, M. F. Zheng, and R. H. Wu *et al.*, “Performance Analysis of Tubular Partitioned Stator Flux-reversal Linear Machine with Different Slot/Pole Combinations and Winding Structures,” *IEEE Trans. on Ind. Appl.*, vol. 58, no. 2, pp. 1991–2000, Mar.–Apr. 2022.
- [45] H. Yang, Z. Q. Zhu, and H. Y. Lin *et al.*, “Synthesis of Hybrid Magnet Memory Machines Having Separate Stators for Traction Applications,” *IEEE Trans. on Veh. Tech.*, vol. 67, no. 11, pp. 183–195, Jan. 2018.
- [46] Z. B. Pan, J. W. Zhao, and S. H. Fang *et al.*, “Topology Development and Performance Analysis of a Dual-stator Permanent Magnet Arc Motor,” *IEEE Trans. on Transport. Electric.*, vol. 9, no. 2, pp. 2509–2523, Jun. 2023.
- [47] Z. B. Pan, S. H. Fang, and H. Wang, “Light GBM Technique and Differential Evolution Algorithm-based Multi-objective Optimization Design of DS-APMM,” *IEEE Trans. on Energy Convers.*, vol. 36, no. 1, pp. 441–455, Mar. 2021.
- [48] Z. B. Pan, and S. H. Fang, “Torque Performance Improvement of Permanent Magnet Arc Motor based on Two-step Strategy,” *IEEE Trans. on Ind. Inform.*, vol. 17, no. 11, pp. 7523–7534, Nov. 2021.
- [49] Z. B. Pan, S. H. Fang, and L. Qin *et al.*, “Research on a Hybrid Excited Arc PM Machine with Partitioned Stator Configuration,” in *Proc. of IEEE Int. Conf. on Appl. Supercond. Electromagn. Devices (ASEMD)*, Tianjin, China, Oct. 2020, pp. 1–2.
- [50] Z. B. Pan, J. W. Zhao, and S. H. Fang *et al.*, “Design and Analysis of a Partitioned-stator Hybrid Excited Permanent Magnet Arc Motor,” in *Proc. of 2024 IEEE International Magnetic Conference-Short papers (INTERMAG Short papers)*, Rio de Janeiro, Brazil, May 2024, pp. 1–2.
- [51] Z. B. Pan, J. W. Zhao, and S. H. Fang *et al.*, “Design and Analysis of a Partitioned-stator Hybrid Excited Permanent Magnet Arc Motor,” *IEEE Trans. on Magn.*, vol. 60, no. 9, pp. 1–6, Sept. 2024.
- [52] Z. B. Pan, and S. H. Fang, “Combined Random Forest and NSGA-II for Optimal Design of Permanent Magnet Arc Motor,” *IEEE J. of Emerg. and Sel. Topics in Power Electron.*, vol. 10, no. 2, pp. 1800–1812, Apr. 2022.
- [53] C. X. Wang, I. Boldea, and S. A. Nasar, “Characterization of Three Phase Flux Reversal Machine as an Automotive Generator,” *IEEE Trans. on Energy Convers.*, vol. 16, no. 1, pp. 74–80, Mar. 2001.
- [54] Y. T. Gao, D. W. Li, and R. H. Qu *et al.*, “Design Procedure of Flux Reversal Permanent Magnet Machines,” *IEEE Trans. on Ind. Appl.*, vol. 53, no. 5, pp. 4232–4241, Sept. 2017.
- [55] Z. B. Pan, J. W. Zhao, and S. H. Fang *et al.*, “Multi-objective Optimization Design of Permanent Magnet Arc Motor based on Gradient Boosting Decision Tree,” in *Proc. of 2023 IEEE Int. Conf. Appl. Supercond. and Electromagn. Devices (ASEMD)*, Tianjin, China, Oct. 2023, pp. 1–2.
- [56] Z. B. Pan, J. W. Zhao, and S. H. Fang *et al.*, “Combined Gradient Boosting Decision Tree and Differential Evolution Algorithm for Optimization Design of Permanent Magnet Arc Motor,” *IEEE Trans. on Appl. Supercond.*, vol. 34, no. 8, pp. 1–5, Nov. 2024.
- [57] Z. B. Pan, S. H. Fang, and H. Wang *et al.*, “Accurate and Efficient Surrogate Model-assisted Optimal Design of Flux Reversal Permanent Magnet Arc Motor,” *IEEE Trans. on Ind. Electron.*, vol. 70, no. 9, pp. 9312–9325, Sept. 2023.
- [58] Z. B. Pan, S. H. Fang, and H. Y. Lin *et al.*, “A New Double-sided Flux Reversal Arc Permanent Magnet Machine with Enhanced Torque Density Capability,” *IEEE Trans. on Magn.*, vol. 55, no. 6, pp. 1–6, Jun. 2019.
- [59] Y. Meng, Y. Z. Zhu, and Y. J. Yu *et al.*, “Comparative Study of New Dual-stator Consequent Pole Flux Reversal Arc PM Machines,” in *Proc. of 2023 IEEE Int. Conf. on Appl. Supercond. and Electromagn. Devices (ASEMD)*, Tianjin, China, Oct. 2023, pp. 1–2.
- [60] Y. Meng, S. H. Fang, and Y. Z. Zhu *et al.*, “Investigation of New Dual-stator Consequent-pole Flux Reversal Permanent Magnet Arc Machines,” *IEEE Trans. on Appl. Supercond.*, vol. 34, no. 8, pp. 1–5, Nov. 2024.
- [61] Z. B. Pan, S. H. Fang, and H. Y. Lin *et al.*, “A New Hybrid-excited Flux Reversal Arc Permanent Magnet Machine Having Partitioned Stators for Large Telescope Application,” *IEEE Trans. on Magn.*, vol. 55, no. 7, pp. 1–10, Jul. 2019.
- [62] Y. T. Gao, D. W. Li, and R. H. Qu *et al.*, “Analysis of a Novel Consequent-pole Flux Switching Permanent Magnet Machine with Flux Bridges in Stator Core,” *IEEE Trans. on Energy Convers.*, vol. 33, no. 4, pp. 2153–2162, Dec. 2018.
- [63] W. Hua, M. Cheng, and G. Zhang, “A Novel Hybrid Excitation Flux-switching Motor for Hybrid Vehicles,” *IEEE Trans. on Magn.*, vol. 45, no. 10, pp. 4728–4731, Oct. 2009.
- [64] Q. F. Lu, Y. H. Yao, and J. M. Shi *et al.*, “Design and Performance Investigation of Novel Linear Switched Flux PM Machines,” *IEEE Trans. on Ind. Appl.*, vol. 53, no. 5, pp. 4590–4602, Sept.–Oct. 2017.
- [65] X. D. Liu, Z. X. Gu, and B. Li *et al.*, “A Novel Cogging Torque Reduction Method for the Modular Arc-linear Flux Switching Permanent-magnet Motor,” in *Proc. of 2016 IEEE Conference on Electromagnetic Field Computation (CEFC)*, Miami, FL, USA, Nov. 2016, pp. 1.
- [66] Z. X. Gu, J. Zhao, and R. Y. Hu *et al.*, “Electromagnetic Structure Research of the Modular Arc-linear Flux Switching Permanent-magnet Motor,” in *Proc. of 2018 21st Int. Conf. on Electr. Mach. and Syst. (ICEMS)*, Jeju, Republic of Korea, Oct. 2018, pp. 1857–1862.
- [67] X. D. Liu, Z. X. Gu, and J. Zhao, “Torque Ripple Reduction of a Novel Modular Arc-linear Flux-switching Permanent-magnet Motor with Rotor Step Skewing,” *Energies*, vol. 9, no. 6, pp. 404–420, May 2016.
- [68] B. Li, J. Zhao, and Q. S. Mou *et al.*, “Research on Torque Characteristics of a Modular Arc-linear Flux Switching Permanent-magnet Motor,” *IEEE Access*, vol. 7, pp. 57312–57320, 2019.
- [69] F. Liu, J. H. Hu, and Y. Li, “Torque and Radial Force Optimization of Arc Flux Switching Permanent Magnet Linear Motor Used for Large Scanning Equipment,” *IEEE Trans. on Energy Convers.*, vol. 37, no. 1, pp. 304–315, Mar. 2022.
- [70] F. Liu, Y. Li, and Y. Xie *et al.*, “A Novel Fault Tolerance Structure of Arc Linear Flux Switching Permanent Magnet Motors based on Redundant Winding,” *IEEE Trans. on Magn.*, vol. 59, no. 11, pp. 1–7, Nov. 2023.
- [71] N. Chen, and S. H. Fang, “A New Torque-enhanced Flux Modulated Permanent Magnet Arc Motor with Flux-concentrated Stator PMs,” in *Proc. of 2023 IEEE Int. Conf. on Appl. Supercond. and Electromagn. Devices (ASEMD)*, Tianjin, China, Oct. 2023, pp. 1–2.
- [72] N. Chen, and S. H. Fang, “Design and Analysis of a Novel Flux Modulated Permanent Magnet Arc Motor with Asymmetric Double-stator,” in *Proc. of IEEE Int. Conf. on Appl. Supercond. and Electromagn. Devices (ASEMD)*, Tianjin, China, Oct. 2023, pp. 1–2.
- [73] N. Chen, and S. H. Fang, “A New Asymmetric Dual-stator Flux Modulated Permanent Magnet Arc Motor for the Drive of Large Telescope Equipment,” *IEEE Trans. on Appl. Supercond.*, vol. 34, no. 8, pp. 1–6, Nov. 2024.
- [74] Q. S. Wang, S. X. Niu, and X. Luo, “A Novel Hybrid Dual-PM Machine Excited by AC with DC Bias for Electric Vehicle Propulsion,”

IEEE Trans. on Ind. Electron., vol. 64, no. 9, pp. 6908–6919, Sept. 2017.

- [75] L. Xu, W. X. Zhao, and G. H. Liu *et al.*, “A Novel Dual-permanent-magnet-excited Machine with Non-uniformly Distributed Permanent-magnets and Flux Modulation Poles on the Stator,” *IEEE Trans. on Veh. Technol.*, vol. 69, no. 7, pp. 7104–7115, Jul. 2020.
- [76] H. L. Huang, D. W. Li, and R. H. Qu *et al.*, “Design and Analysis of T-shaped Consequent Pole Dual PM Vernier Machines with Differential Magnetic Network Method,” *IEEE J. of Emerg. and Sel. Topics in Power Electron.*, vol. 10, no. 4, pp. 4546–4555, Aug. 2022.
- [77] Q. F. Lin, S. X. Niu, and F. B. Cai *et al.*, “Magnet Eddy Current Loss and Thermal Analysis of a Dual-permanent-magnet-excited Machines,” *IEEE J. of Emerg. and Sel. Topics in Power Electron.* vol. 10, no. 4, pp. 3793–3804, Aug. 2022.
- [78] Z. B. Pan, S. H. Fang, and L. Qin *et al.*, “Design and Analysis of Variable Flux Arc Permanent Magnet Motor with Multiple Excitations,” *IEEE Trans. on Magn.*, vol. 57, no. 6, pp. 1–5, Jun. 2021.
- [79] K. W. Wei, Z. B. Pan, and J. W. Zhao *et al.*, “Topology Design and Performance Analysis of a New Dual-PM Excited Permanent Magnet Arc Motor,” in *Proc. of 2023 26th Int. Conf. on Electr. Mach. and Syst. (ICEMS)*, Zhuhai, China, Nov. 2023, pp. 1400–1403.
- [80] K. W. Wei, Z. B. Pan, and J. W. Zhao *et al.*, “Design and Analysis of a Multiunit Distributed Permanent Magnet Arc Motor Having Double-sided Permanent Magnet Excitations,” *IEEE Trans. on Transport. Electric.*, vol. 11, no. 1, pp. 1177–1188, Feb. 2025.
- [81] J. Y. Wang, D. M. Huang, and S. H. Fang *et al.*, “Model Predictive Control for ARC Motors Using Extended State Observer and Iterative Learning Methods,” *IEEE Trans. on Energy Convers.*, vol. 37, no. 3, pp. 2217–2226, Sept. 2022.
- [82] D. M. Huang, S. H. Fang, and Z. B. Pan *et al.*, “Low-speed Model Predictive Control based on Modified Extended State Observer of Arc Motor,” *IEEE Trans. on Ind. Electron.*, vol. 70, no. 7, pp. 6675–6685, Jul. 2023.
- [83] X. L. Song, and Z. J. Cao, “Research on Control Strategy of Hamiltonian Theory for Large Telescope based on SAPMSM,” *IEEE Access*, vol. 12, pp. 31960–31967, Mar. 2024.
- [84] D. M. Huang, S. H. Fang, and Q. R. Xu, “A Position-tracking Method for Arc Motor based on Iterative Learning Super-twisting Observer and Super-twisting Control,” *IEEE J. of Emerg. and Sel. Topics in Power Electron.*, vol. 13, no. 2, pp. 2200–2210, Apr. 2025.
- [85] S. H. Fang, Y. T. He, and P. Wan *et al.*, “Low-speed Control of Arc Motor Using Kalman Observer Via Acceleration-based Disturbance Observer,” *IEEE Trans. on Power Electron.*, vol. 39, no. 1, pp. 1254–1268, Jan. 2024.
- [86] Q. R. Xu, S. H. Fang, and P. Wan *et al.*, “Low-speed LADRC for Permanent Magnet Synchronous Motor with High-pass Speed Compensator,” *IEEE J. of Emerg. and Sel. Topics in Power Electron.*, vol. 11, no. 6, pp. 6016–6027, Dec. 2023.
- [87] Z. B. Pan, J. W. Zhao, and K. W. Wei *et al.*, “Design and Analysis of Permanent Magnet Arc-linear Motor Having Different Stator-permanent Magnet Arrangements,” *IEEE Trans. on Plasma Sci.*, vol. 53, no. 3, pp. 430–438, Mar. 2025.



Zhenbao Pan (Member, IEEE) was born in Guilin, China. He received the B.S. degree in Electrical Engineering and Automation from Anhui University, Hefei, China, in 2014, the M.S. degree in Detection Technology and Automatic Equipment from Anhui University, Hefei, China, in 2017, and the Ph.D. degree in

Electrical Engineering from Southeast University, Nanjing, China, in 2022.

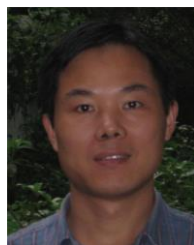
Since 2022, he has been with Hefei University of Technology, where he is currently a Lecturer with the School

of Electrical Engineering and Automation. From 2023 to 2025, he was a Postdoctoral Scholar with the Hefei University of Technology and Whirlpool (China) Co., Ltd. His main research interests include design, optimization and control of permanent-magnet motors with particular reference to permanent-magnet linear motors and permanent-magnet arc motors.



Jiwen Zhao (Senior Member, IEEE) was born in Dangshan, China. He received his Ph.D. degree in 2005 from University of Science and Technology of China, Hefei, China.

Since 2019, he has been working with the School of Electrical and Automation Engineering, Hefei University of Technology, Hefei, China. Now he is a professor in the School of Electrical and Automation Engineering, Hefei University of Technology, Hefei. His main research interests include PM linear motor optimization design, control and photoelectric detection technology.



Shuhua Fang (Senior Member, IEEE) received the M.S. degree from Shandong University of Science and Technology, Jinan, China, and the Ph. D. degree from Southeast University, Nanjing, China, in 2004 and 2008, respectively, both in electrical engineering.

From 1998 to 2001, he was an Associate Engineer with the Xuzhou Coal and Mine Machinery Factory, Xuzhou, China, where his research activities were primarily in the area of the design, analysis, and control of electrical apparatus. Since 2008, he has been with Southeast University, where he is currently a full Professor with the School of Electrical Engineering. From 2013 to 2014, he was a Visiting Professor at the Wisconsin Electric Machines and Power Electronics Consortium (WEMPEC), University of Wisconsin-Madison, Madison, WI, USA. His research interests include design, simulation, and control for both permanent-magnet actuators and intelligent apparatus.



Jinhao Cai was born in Chizhou, Anhui, China. He received the B.S. degree in Electrical Engineering and Automation from Tiangong University, Tianjin, China, in 2023. Since 2023, he is currently working toward the M.S. degree in the School of Electrical Engineering and Automation, Hefei University of

Technology, Hefei, China.

His current research interests include the structural design, analysis, and optimization of the permanent-magnet arc motors.



Qiangren Xu (Graduate Student Member, IEEE) received the B.Eng. degree in electrical engineering and automation from Southeast University, Nanjing, China, in 2019, and the M.Eng. degree aeronautical and astronautical science and technology from the Shanghai Academy of Spaceflight Technology, Shanghai, China, in 2022. He is currently working toward the Ph.D. degree in electrical engineering at Southeast University.

His research interests include control strategies for permanent magnet machines and power electronics.